



1 The Impact of Climate on Surging at Donjek Glacier, Yukon, Canada

2

3 William Kochtitzky^{1,2}, Dominic Winski^{1,2}, Erin McConnell^{1,2}, Karl Kreutz^{1,2}, Seth Campbell^{1,2},
4 Ellyn M. Enderlin^{1,2,3}, Luke Copland⁴, Scott Williamson⁴, Brittany Main⁴, Christine Dow⁵,
5 Hester Jiskoot⁶

6

7 ¹*School of Earth and Climate Sciences, University of Maine, Orono, Maine, USA*

8 ²*Climate Change Institute, University of Maine, Orono, Maine, USA*

9 ³*Department of Geosciences, Boise State University, Boise, Idaho, USA*

10 ⁴*Department of Geography, Environment and Geomatics, University of Ottawa, Ottawa, ON,*
11 *Canada*

12 ⁵*Department of Geography and Environmental Management, University of Waterloo, Waterloo,*
13 *ON, Canada*

14 ⁶*Department of Geography, University of Lethbridge, Lethbridge, AB, Canada*

15

16 *Correspondence to:* William Kochtitzky (william.kochtitzky@maine.edu)

17 **Abstract.** Links between climate and glacier surges are not well understood, but are required to
18 enable prediction of glacier surges and mitigation of associated hazards. Here, we investigate the
19 role of snow accumulation and temperature on surge periodicity, glacier area changes, and
20 timing of surge initiation since the 1930s for Donjek Glacier, Yukon, Canada. Snow
21 accumulation measured in three ice cores collected at Eclipse Icefield, at the head of the glacier,
22 indicate that a cumulative accumulation of 13.1-17.7 m w.e. of snow occurred in the 10-12 years
23 between each of its last eight surges. This suggests that a cumulative accumulation threshold
24 must be passed before the initiation of a surge event, although it remains unclear whether the
25 relationship between cumulative snowfall and surging is due to the consistency in repeat surge
26 interval and decadal average precipitation, or if it is indeed a prerequisite to surging. We also
27 examined the 1968 to 2017 climate record from Burwash Landing, 30 km from the glacier, to
28 determine whether a relationship exists between surge periodicity and an increase of 2.5°C in
29 mean annual air temperature over this period. No such relationship was found, although each of
30 the past 8 surge events has been less extensive than the previous, with the terminus area
31 approximately 7.96 km² smaller after the 2012-2014 surge event compared to the ~1947 surge
32 event. This study shows that the impacts of climate and surging is not yet understood and
33 suggests that internal glacier processes may play a more important role in controlling glacier
34 surge events.

35

36 **1. Introduction**



37 Surge-type glaciers account for ~1% of glaciers globally (Sevestre and Benn, 2015), but can be
38 the dominant glacier type in some regions (e.g., Clarke et al., 1986; Jiskoot et al., 2003), and are
39 important for understanding ice flow instabilities and anomalous glacier response to climate
40 change (Yde and Paasche, 2010). Surge-type glaciers have long periods of flow at rates below
41 their balance velocity (quiescent phase), typically on the order of decades, which are interrupted
42 by short-lived phases of glacier flow at rates much higher than the balance velocity (active phase
43 or surge phase), typically on the order of months to years, that are driven by internal instabilities
44 and sometimes lead to a marked frontal advance (Meier and Post, 1969; Clarke, 1987). When a
45 glacier surges, its reservoir zone at higher elevations loses mass and its receiving zone at lower
46 elevations gains mass, with the line of zero net mass change defined as the dynamic balance line
47 (DBL: Dolgoushin and Osipova, 1975). When mass gain in the receiving zone leads to a
48 significant advance of the terminus, an increased calving flux or other proglacial hazards can
49 occur.

50 Surges of temperate glaciers are typically hypothesized to initiate when a critical basal
51 shear stress is reached in a surge initiation region, causing the subglacial hydrologic system to
52 reorganize and the glacier to rapidly redistribute its accumulated mass down-glacier (Meier and
53 Post, 1969; Raymond, 1987; Eisen et al., 2005). While this hydrologic mechanism dominates
54 Yukon-Alaska type surging, a thermal triggering mechanism (i.e., surging controlled by basal ice
55 temperature), or combined hydro-thermodynamic mechanism, has been documented in surges of
56 polar and polythermal glaciers, such as those in Svalbard and smaller glaciers in Yukon-Alaska
57 (Murray et al., 2003; Frappé and Clarke, 2007; De Paoli and Flowers, 2009; Dunse et al., 2015).
58 Finally, overarching theories related to balance flux (Budd, 1975) and enthalpy (Sevestre et al.,
59 2015) have been proposed as well.

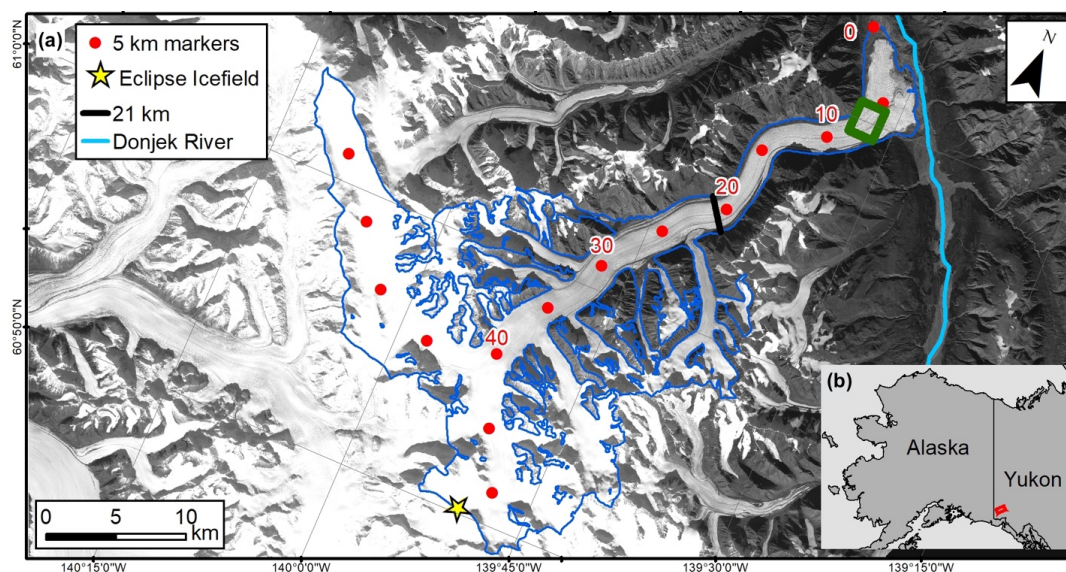
60 The length of a surge cycle (i.e., combined quiescent and active phases) is typically
61 consistent for an individual glacier, and is proportional to the length of the surge phase (Meier
62 and Post, 1969; Dowdeswell and others, 1991). In turn, quiescence duration is controlled by
63 mass balance conditions (Robin and Weertman, 1973), meaning that surge periodicity is
64 inversely related to accumulation rates (Dyurgerov *et al.*, 1985; Osipova and Tsvetkov, 1991;
65 Dowdeswell *et al.*, 1991). Prolonged quiescent phases (decades to centuries) typical of the
66 Svalbard region have been ascribed to low accumulation rates, often only on the order of 0.3-0.6
67 m a^{-1} (Dowdeswell *et al.*, 1995), while short repeat intervals (12-20 years) on Variegated Glacier,



68 AK, correspond to accumulation rates on the order of 1.4 m a^{-1} (Eisen et al., 2001; Van Geffen
69 and Oerlemans, 2017). However, there can be large variations in surge periodicity between
70 glaciers in the same region. For example, Icelandic glaciers have irregular quiescent intervals, 5-
71 30 years for some glaciers and up to 100-140 for others (Björnsson et al., 2003; Sigurdsson,
72 2005).

73 Changes in surge recurrence interval has been linked to changing cumulative mass
74 balance (Dowdeswell et al., 1995; Copland et al., 2011; Eisen et al., 2001; Striberger et al.,
75 2011). Dowdeswell et al. (1995) found a persistent negative mass balance reduced the glacier
76 surge activity in Svalbard. Conversely, an increase in precipitation and positive glacier mass
77 balance on Karakoram glaciers is associated with an elevated number of surge events, although it
78 is unclear whether the increase in accumulation (Copland et al., 2011) or increase in intense
79 short-term melting periods Hewitt (2007) drove the increase in surging. Eisen et al. (2001)
80 reported a variable surge recurrence interval that was consistent with changing amounts of
81 precipitation on Variegated Glacier, Alaska. Similarly, Striberger et al. (2011) found a variable
82 surge repeat interval at Eyjabakkajökull, Iceland associated with changes in climatically-driven
83 mass balance.

84 Previous efforts to examine connections between cumulative snow accumulation and
85 length of the quiescent phase have used mass balance models, off-ice meteorological
86 measurements, and a limited record of in situ mass balance measurements (Eisen et al., 2001;
87 Tangborn, 2013; Dyurgerov et al., 1985). Although these studies found that a snow accumulation
88 threshold had to be reached before each surge started, this potential linkage has not yet been
89 tested with observations of glacier surface mass balance. Here, we use the well-documented
90 history of surge events at Donjek Glacier (Abe et al., 2016; Kochtitzky et al., In Review; Fig. 1),
91 and ice cores extracted from Eclipse Icefield at the head of the glacier (Wake et al., 2002; Yalcin
92 et al., 2006; Kelsey et al., 2012), to explore linkages between snow accumulation and surging
93 since the 1930s. We combine these observations with weather station records, digital elevation
94 models, and remote sensing analysis to examine the impacts of climate and ice kinematics on
95 surge behavior. The combination of data from eight surge events and three independent ice core
96 records in the accumulation zone, make Donjek Glacier an ideal site to test the influence of
97 climate on surge behavior.



98
99 Figure 1. (a) Donjek Glacier (blue outline; RGI Consortium, 2017), with Eclipse Icefield marked
100 with the yellow star and Donjek River in light blue. Black line indicates the separation between
101 the downglacier surge-type and upglacier non-surge-type portions of the glacier. Green box
102 indicates extent of Figure 7a. (b) Location of Donjek Glacier in southwestern Yukon; red box
103 indicates extent of a. Base image from Landsat 8, 23 September, 2017.

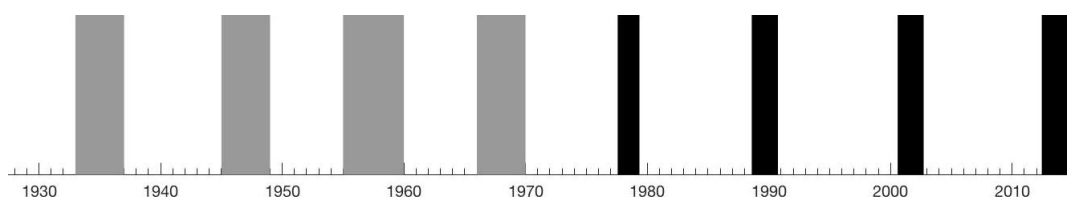
104

105 2. Study Site

106 Donjek Glacier (61°11'N, 139°31'W; Figure 1) is a surge-type glacier located in southwest
107 Yukon in the St. Elias Mountains. In 2010, Donjek Glacier was 65 km long with a surface area
108 of 448 km² (RGI Consortium, 2017). While the Tlingit indigenous peoples of the Yukon were
109 the first to observe Donjek Glacier surge (Cruikshank, 1981), the first scientific records are from
110 1937 in the form of Bradford Washburn's air photos (<https://library.uaf.edu/washburn/>).
111 Subsequent scientific work focused on the moraines and geomorphology (Denton and Stuvier,
112 1966; Johnson, 1972a and b), meteorological measurements at Eclipse Icefield as part of the
113 Icefield Ranges Research Project (Ragle, 1972), and surge-related outburst floods in the Donjek
114 River (Figure 1; Clarke and Mathews, 1981). Ice coring campaigns have occurred at least four
115 times at Eclipse Icefield since the 1990s and provide a wealth of snow accumulation and
116 atmospheric information (Wake et al., 2002; Yalcin et al., 2006; Kelsey et al., 2012).



117 Between May 2000 and May 2012, the area-averaged mass balance of Donjek Glacier
118 was -0.29 m water equivalent (w.e.) yr^{-1} , or -0.13 Gt yr^{-1} (Larsen et al., 2015). Despite this
119 negative mass balance, the glacier has continued its history of frequent surging, which has
120 occurred approximately every 10-12 years since the 1930s (Abe et al., 2016; Kochtitzky et al., In
121 Review; Figure 2). Air photo records, satellite imagery and previous reports indicate that the
122 glacier surged in ~ 1935 , ~ 1947 , late-1950s, ~ 1969 , 1977-1980, 1988-1990, 2000-2002, and
123 2012-2014, with progressively less extensive terminus advances up to the present day. Ice flow
124 velocities are only available for the two most recent surges (Abe et al., 2016; Kochtitzky et al., In
125 Review). Only the lower 21 km of the glacier was involved in these surge events, coinciding
126 with the portion of the glacier down-glacier of a valley constriction (Kochtitzky et al., In
127 Review; Figure 1).



128
129 Figure 2. Surge event timing. Grey bars indicate uncertainty for surges before the satellite era.
130 Black bars indicate duration of active surge phase for the last four surge events, constrained by
131 satellite imagery.

132

133 3. Methods

134 3.1. Ice cores and snow accumulation record

135 Ice cores were collected at Eclipse Icefield (Fig. 1) in 1996 (160 m absolute length; Yalcin and
136 Wake, 2001), 2002 (350 m absolute length; Fisher et al., 2004; Kelsey et al., 2012), and 2016 (59
137 m absolute length), to develop an understanding of past climate in the St. Elias Range. Cores
138 were collected during late spring, but preceding the melt season, in 1 m segments using a 8.2 cm
139 diameter electromechanical drill. The accumulation record from the 1996 ice core was originally
140 reported by Yalcin and Wake (2001) and we use their original data here. An original depth-age
141 scale for the 2002 core was developed by Yalcin et al. (2007). Since then, advances in
142 glaciochemical signal detection, automated layer counting (Winstrup et al., 2012), and ice flow
143 modeling have been developed for alpine ice cores (Campbell et al., 2013; Winski et al., 2017).
144 We therefore applied these techniques to the existing Eclipse 2002 core data to develop updated

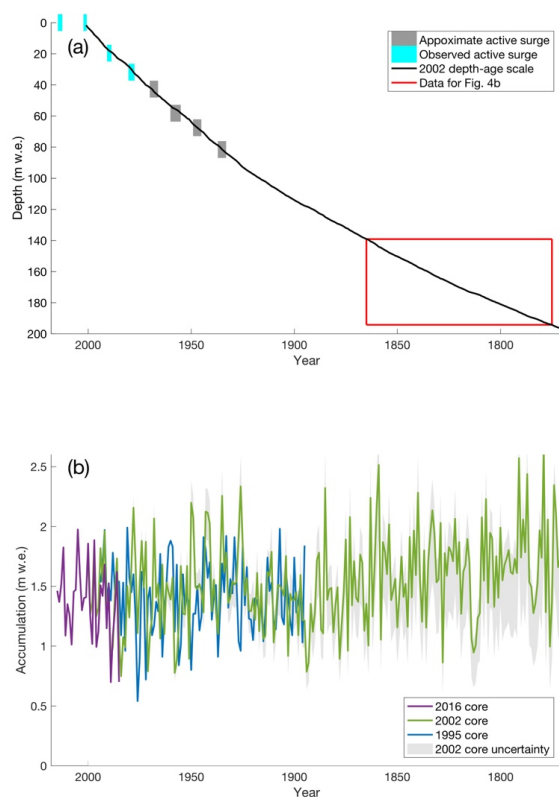


145 accumulation rate time series. The 2016 core was primarily dated using oxygen ($\delta^{15}\text{O}$) and
146 deuterium (δD) isotope ratios, and deuterium excess (d_{xs} ; equation 1; Dansgaard, 1964), with
147 additional constraints from major ions (Na^+ , SO_4^{2-} , and Mg^{2+}). We do not apply any thinning
148 corrections to the 2016 core, as it only covers the top 59 m of the firn zone and firn/ice transition
149 where thinning is negligible. The 2002 core was dated via annual layer counting of δD , sodium,
150 magnesium, calcium, and sulfate. The 2002 core was additionally constrained by known volcanic
151 eruption markers indicated by a spike in sulfate concentrations (Yalcin et al., 2007) and the Cs-
152 137 peak in 1963 from above ground nuclear testing. The seasonal timing of each of these peaks
153 is well characterized from previous studies in the North Pacific region (Yalcin et al. 2001, Wake
154 et al. 2002, Yasunari et al. 2007, Osterberg et al. 2014, Winski et al. 2017).

$$155 \quad d_{xs} = \delta\text{D} - 8 \times \delta^{15}\text{O} \quad (1)$$

156 Five individuals independently picked the approximate position of the 1 January marker
157 throughout the last 500 years for the 2002 ice core (Fig. 3a). These individual annual pick
158 positions were reconciled using the methods described in Winski et al. (2017), which included
159 incorporation of algorithm-based computer counting software (Winstrup et al., 2018). With the
160 resulting annually-dated timescale, annual layer thicknesses were calculated as the distance
161 between successive years, and water equivalent annual layer thicknesses were calculated as the
162 annual layer thickness multiplied by the density at the corresponding depth in the ice core. The
163 density for each layer was extrapolated from the 1 m-increment field density measurements.

164 We accounted for thinning due to glacier flow in the 2002 record using three 1-
165 dimensional glacier flow models, which we refer to as the Nye (Nye, 1963), Hooke (Kaspari et
166 al. 2008), and Dansgaard-Johnsen (Dansgaard and Johnsen, 1969) models (Fig. 3b). Following
167 Winski et al. (2017), we tested all reasonable combinations of free parameters in each model to
168 assess which model run most closely matches our observed depth-age scale (Fig. 3a). In each
169 model, we generated a suite of different age scales using long-term average accumulation rates
170 ranging from 20 to 300 cm in 10 cm increments. In the Hooke model, we also permitted the flow
171 parameter (m in Kaspari et al. 2008) to vary between 1 and 2. In the Dansgaard-Johnsen model
172 we permitted a flow regime change occurring between 10 and 250 m above the bed. These
173 activities resulted in a total of 1363 separate model runs (29 Nye, 609 Hooke and 725
174 Dansgaard-Johnsen), each producing a unique depth age scale.



175
176 Figure 3. Ice core accumulation and depth-age scale. (a) The mean picked observed depth-age
177 scale from the 2002 ice core is shown in black with grey lines indicating each of the individual
178 picks. (b) The 1995 ice core (purple), 2002 ice core (green), and 2016 ice core (blue)
179 accumulation records are shown since 1770. The Nye and Hooke models are the bounds on the
180 2002 ice core uncertainty (grey) for accumulation from the 2002 ice core.

181
182 For each modeled depth age scale, we calculated the sum of root-mean squared errors
183 (RMSE) between the layer-counted and modeled depth-age scale positions at each year. Of all
184 combinations of models and input parameters, we found the optimized version of the Dansgaard-
185 Johnsen Model to produce the lowest RMSE and closest match to our observed depth-age scale.
186 In our modeled depth-age scale, we used 337 m w.e. (approximately 376 m of absolute
187 thickness) which yielded the lowest error between the optimized Dansgaard-Johnsen model (the



188 closest fit) and the layer counted timescale. The accumulation rate used herein is equal to the
189 ratio of the observed layer thickness (from the annual layer counting) over the modeled layer
190 thickness (from the optimized Dansgaard-Johnsen model) multiplied by 1.4 meters, which is the
191 optimized value of long-term accumulation that produces the best fit to the timescale. Based on
192 the range of results among the three flow models, the accumulation uncertainty was estimated as
193 $\pm 15\%$ in the 1930s, with lower uncertainties near the top of the record.

194 We define our cumulative accumulation interval for each quiescent phase to stretch from
195 the year following surge initiation to the initiation year of the next surge (Eisen et al., 2001),
196 which equates to 1935-1944, 1945-1955, 1956-1966, 1967-1977, 1978-1988, 1989-2000, and
197 2001-2012 (Fig. 2). The surge initiation dates we use are from Kochtitzky et al. (In Review),
198 which are well constrained in the satellite era. Before the satellite era, our initiation years are
199 within the uncertainty bounds determined by Kochtitzky et al. (In Review) from advanced
200 terminus positions and/or push moraines captured in air photographs.

201

202 **3.2. Glacier surface elevation mapping**

203 Digital Elevation Models (DEMs) for 2002, 2007, 2012, and 2016 were created or obtained from
204 Operation IceBridge (OIB) LiDAR measurements, Satellite Pour l'Observation de la Terre 5
205 (SPOT-5), WorldView and the Advanced Spaceborne Thermal Emission and Reflection
206 Radiometer (ASTER; Table 1). OIB LiDAR tracks from 2012 and 2016 were downloaded from
207 the National Snow and Ice Data Center (<https://nsidc.org/icebridge/portal>) and down-sampled to
208 8 m spatial resolution for comparison with the DEMs. We obtained a 13 September 2007 SPOT-
209 5 DEM (40 m spatial resolution) from the SPIRIT Project (<https://theia-landsat.cnes.fr>) with an
210 uncertainty of ± 6 m (Korona and others, 2009). We received DEMs at 8 m spatial resolution
211 derived from WorldView imagery from the University of Minnesota Polar Geospatial Center
212 (PGC), with ~ 0.2 m vertical accuracy (Shean and others, 2016). We mosaicked the individual
213 WorldView DEMs from 10 August and 27 September 2013 (hereby referred to as the
214 August/September 2013 DEM) to create a more spatially extensive DEM of the glacier. These
215 2013 DEM strips do not overlap or intersect, so we are unable to quantify the potential aliasing
216 of glacier flow and/or melt in the mosaicked DEM. Finally, we created one 2002 DEM from
217 ASTER imagery using MMASTER from Girod and others (2017). The ASTER DEM has 30 m
218 spatial resolution and 10 m vertical uncertainty (Girod and others, 2017). We co-registered all



219 DEMs to the WorldView DEMs following methods from Nuth and Kääb (2011) and smoothed
220 extracted centerline elevation values using a 300 m moving window to visualize the data.
221 Table 1. Elevation data sources for ice surface change

Source	Date	Vertical uncertainty
ASTER (satellite)	26/05/2002	10 m
SPOT-5 (satellite)	13/09/ 2007	6 m
Operation IceBridge (airborne LiDAR)	22/05/2012 15/05/2016	<10 cm
PGC/WorldView (satellite)	10/08/2013 27/09/2013	~0.2 m

222

223 3.3. Snowline measurements

224 To infer the position of the equilibrium line altitude, we manually digitized the position of the
225 snowline using the Landsat archive. All available cloud-free Landsat images of Donjek Glacier
226 were downloaded from Earth Explorer (<https://earthexplorer.usgs.gov>), and the last available
227 image of the ablation season (July, August, or September) of each year was selected to determine
228 the snowline for most years from 1972-2017. We additionally used one air photo from 8 July
229 1951, which we georeferenced with 8 tie points to produce an estimated horizontal uncertainty of
230 72.4 m.

231 We estimated the mean elevation of the snowline for each year using a 2013 WorldView
232 DEM (see section 3.4). We are unable to account for glacier surface elevation change over time
233 due to a lack of high-quality surface DEMs prior to 2002, but little change (less than 30 m) in
234 exposed rock along the glacier margins since the 1970s suggests that elevation changes have not
235 been large.

236

237 3.4 Ice thickness measurements

238 During a July, 2018 field campaign we measured ice thickness by walking with a ground
239 penetrating radar from Blue System Integration Ltd. (<http://www.radar.bluesystem.ca/>) with 5
240 and 10 MHz antennas to measure ice thickness over the lower ablation area of Donjek Glacier in



241 July 2018. Data were processed using IceRadarAnalyzer 4.2.5, assuming a radio-wave velocity
242 of 0.300 m ns^{-1} in air and 0.170 m ns^{-1} in ice (Mingo and Flowers, 2010).

243

244 **3.5. Climate and weather observations**

245 To infer climate conditions at Donjek Glacier, we use temperature and precipitation data from
246 the Environment and Climate Change Canada weather station at Burwash Landing ($61^{\circ}22'14''\text{N}$,
247 $139^{\circ}2'24''\text{W}$, 806 m a.s.l.), 30 km northeast of the current glacier terminus ($\sim 1000 \text{ m a.s.l.}$). Data
248 were downloaded from <http://climate.weather.gc.ca> using the Canadian Climate Data Scraping
249 Tool (Bonifacio et al., 2015). The Burwash Landing weather station has been operational since
250 1968 and has a nearly continuous hourly and daily record. We do not apply an elevation
251 correction to any weather data from Burwash Landing since we are using these data to infer
252 relative changes over time.

253 We constructed a continuous annual mean temperature record from monthly average
254 temperatures recorded at the weather station to examine long-term temperature change. We also
255 reconstructed a record of annual positive degree days (PDD) from the daily temperature data
256 from Burwash Landing (e.g., Ohmura, 2001). Of the 18,263 day record from 1 January 1968 to
257 31 December 2017, 1038 days did not have mean daily temperature readings. To fill these gaps,
258 we linearly interpolated missing data using the daily mean temperature observation nearest in
259 time. We then calculated the number of annual positive degree days by summing the daily mean
260 temperature for all days that exceeded 0°C for each calendar year.

261 We summed daily rainfall data from Burwash Landing to calculate annual liquid
262 precipitation. 2479 days of daily data are missing, of which 1010 occur between May 1 and
263 September 30, but we do not attempt to fill these, so annual estimates should be considered as
264 minima and are biased based on when observations occurred. The precipitation data cover
265 October 1966 to January 2013. These data allow us to examine the impacts of cumulative and
266 extreme rain events.

267 To complement the Burwash Landing station observations and provide a temperature
268 record on Donjek Glacier, we use the North American Regional Re-analysis (NARR) data set
269 produced by the National Center for Environmental Prediction (NCEP). NARR air temperatures
270 are produced through the combination of surface, radiosonde, and satellite temperature data with
271 the Eta atmospheric model (Mesinger et al., 2006). The surface air temperatures at three-hour



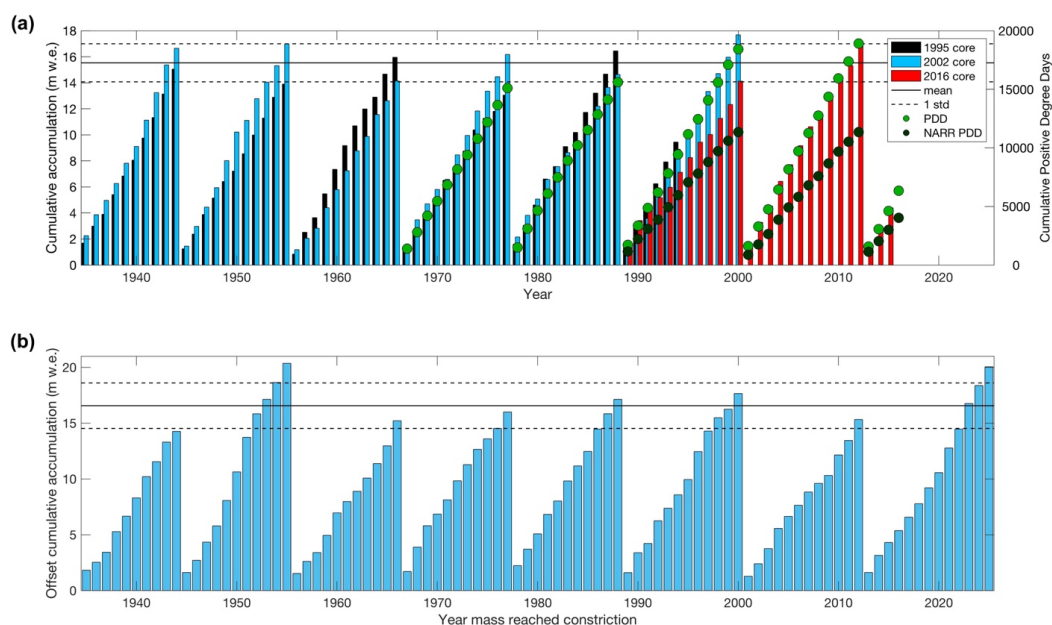
272 intervals for June, July and August over the period 2000 to 2016, were downscaled using
273 atmospheric temperatures from 16 pressure levels between 1000 hPa and 500 hPa (Jarosch et
274 al., 2012). The NARR air temperatures were downscaled to a resolution of 200 m, from the native
275 32 km, using a three-part, linear piece-wise fitting to vertical air profiles and interpolation of the
276 fitted parameters. The downscaled NARR air temperatures perform as well in the Yukon St.
277 Elias region as over British Columbia, which has been confirmed with meteorological air
278 temperature measurements and MODIS Land Surface Temperature measurements over regions
279 of permanent snow and ice (Williamson et al., 2017, Williamson et al., 2018). The 200 m
280 downscale produced a mean bias of 0.5°C and a mean absolute error $\leq 2^\circ\text{C}$ for monthly averages
281 compared to 78 stations in southern British Columbia for data between 1990 and 2008 (Jarosch
282 et al., 2012). We produced daily averages from the 3-hourly downscaled NARR product and
283 subset the data into 200 m elevation bins for Donjek Glacier using the Randolph Glacier
284 Inventory glacier outline. To calculate the PDDs we summed the daily averages higher than 0°C
285 for May through September between 1979 and 2016.

286

287 **4. Results**

288 **4.1 Cumulative accumulation**

289 Using the cumulative annual snow accumulation from the three ice cores, we find that between
290 13.1 and 17.7 m w.e. (mean of 15.5 ± 1.46 m w.e.) accumulated at Eclipse Icefield between each
291 of the eight recent surges of Donjek Glacier (Figure 4a). While the three ice cores do not record
292 the same amount of accumulation each year, they also do not show a pattern of consistent spatial
293 bias of snow accumulation across Eclipse Icefield when compared to each other (Fig. 3).



294

295 Figure 4. Cumulative accumulation between surge events. (a) Cumulative annual accumulation
 296 from 1995 (black), 2002 (blue), and 2016 (red) ice cores between each surge event. Green
 297 (Burwash Landing) and black (NARR) circles indicate cumulative positive degree days between
 298 surge events on the right y-axis. (b) The cumulative accumulation from the 2002 ice core
 299 by 160 years, the time need for surface snow/firn/ice to travel from Eclipse Icefield to the
 300 constriction at 21 km from the terminus, where the surge-type portion of the glacier begins. Solid
 301 and dashed black lines show the mean and one standard deviation cumulative accumulation
 302 average between surge events.

303

304 Surging is limited to the lower 21 km of Donjek Glacier (Kochtitzky et al., In Review;
 305 Figure 1), with the upper boundary of the reservoir zone coinciding with a valley constriction.
 306 Therefore, snow accumulation 32.3 km upstream of the constriction may not have a strong
 307 influence on surge behavior. We therefore calculated the time that it would take mass to advect
 308 from Eclipse Icefield to the constriction from the surface flow speed, neglecting ablation and any
 309 submergence or emergence velocity. In 2007, the average surface flow speed was 201.4 m a^{-1}
 310 along the entire length of Donjek Glacier's center flowline, with a spatial variability of $11.4 -$
 311 398 m yr^{-1} over the 32.3 km trajectory between the ice cores and the constriction (Van Wychen
 312 et al., 2018). Thus, snow that accumulates on Eclipse Icefield takes ~ 160 years to reach the

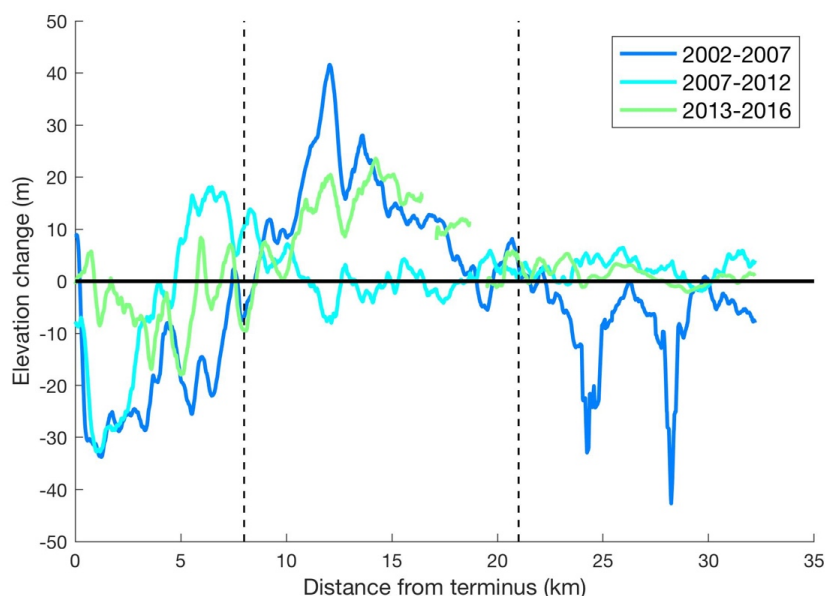


313 constriction, assuming that present-day velocities are similar to those of the past. We therefore
314 offset the accumulation record derived from the 2002 ice core by 160 years to reconstruct the
315 accumulation history preceding the surges (e.g. accumulation that reached the constriction in
316 2002 fell as snow in 1842; Figure 3). Using this offset record, the cumulative accumulation
317 between the eight surge events ranges between 14.2 and 20.4 m w.e. (mean of 16.6 ± 2.0 m w.e.;
318 Figure 4b). Although this results in only a marginally wider range than the recent accumulation
319 history, the average cumulative accumulation is 6% lower.

320

321 **4.2 Changes in the reservoir zone surface height**

322 Donjek Glacier can be divided into two parts: surge-type and non-surge-type (Kochtitzky et al.,
323 In Review). The surge-type portion can further be divided into a reservoir zone (8-21 km
324 upstream of terminus) and a receiving zone (lower 8 km). The area separating the reservoir and
325 receiving zones, which is the area with zero net mass change during a surge event, is known as
326 the dynamic balance line (DBL: Dolgoushin and Osipova, 1975). Our surface DEM analysis
327 demonstrates that surface elevation increases in the reservoir zone following a surge event, even
328 though the entire reservoir zone is located in Donjek Glacier's ablation area. Between 2002 and
329 2007, after the 2000-2002 surge, we measured a glacier surface height increase of up to 41.6
330 ± 11.6 m in the 8-21 km reservoir zone, with an average height increase of 12.5 m (Figure 5).
331 From 2007-2012, covering the beginning of the 2012-2014 surge, the reservoir zone had an
332 average surface elevation increase of 1.0 m (Figure 5). During the surge event, the reservoir zone
333 decreased in surface elevation (Kochtitzky et al., In Review). From 2013-2016, a period which
334 includes the end of the 2012-2014 surge event, we measured an average surface elevation
335 increase of 10.7 m in the reservoir zone (Figure 5). After both the 2000-2002 and 2012-2014
336 surge events, we see refilling of the reservoir zone within five years (Figure 5).



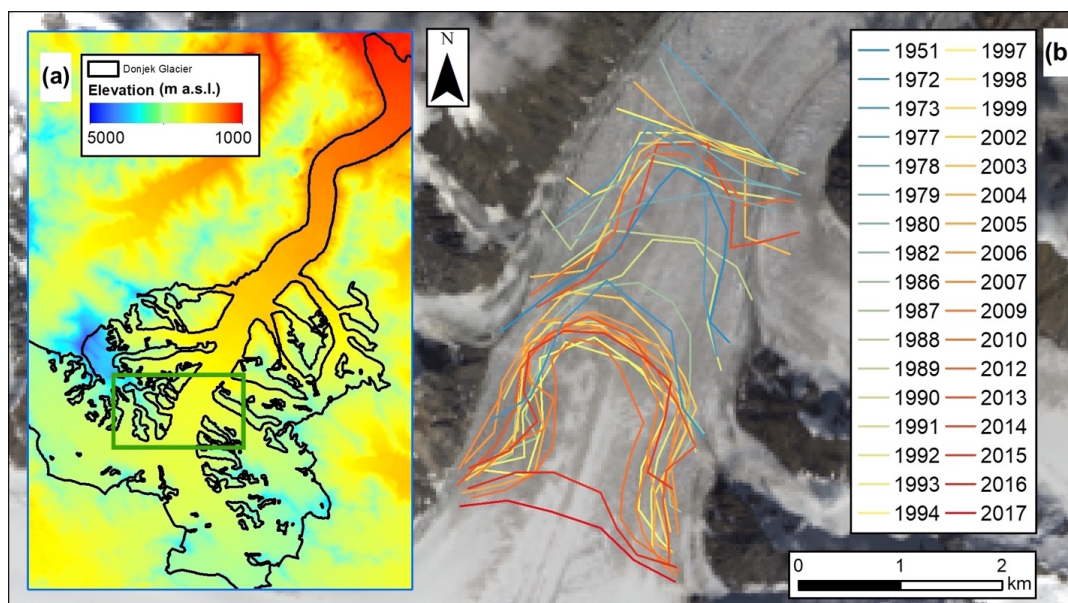
337

338 Figure 5. Surface elevation change in the reservoir zone. Surface elevation change from 2002 to
339 2007 (dark blue), 2007 to 2012 (light blue), and 2013 to 2016 (light green). Extent of the
340 reservoir zone indicated by black dashed lines at 8 km (dynamic balance line) and 21 km
341 (constriction) from the terminus.

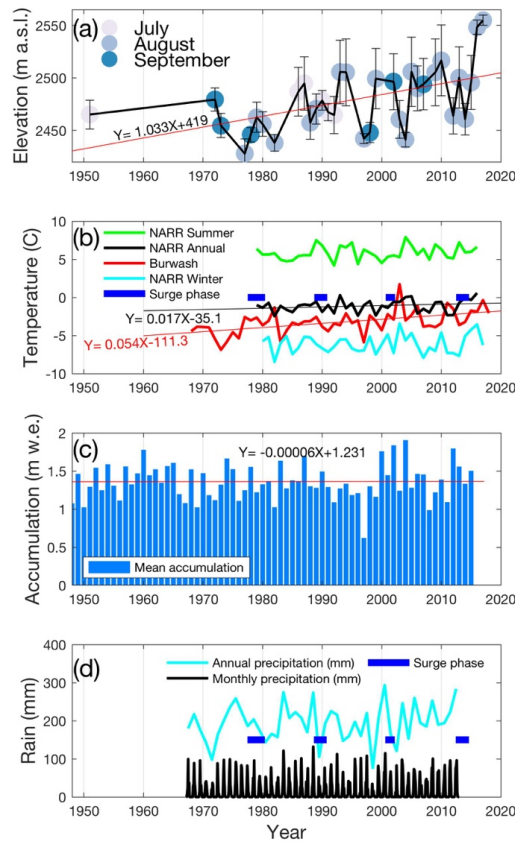
342

343 4.3 Snowline change

344 Our remote sensing analysis illustrates that the summer snowline in the center flow unit of
345 Donjek Glacier has migrated up-glacier by 55 m yr^{-1} horizontally and risen by $\sim 1.0 \text{ m yr}^{-1}$ in
346 elevation over the period 1951 to 2017 (Figures 6 and 7a). Over the study period the snowline
347 was lowest in 1977 (Figure 7a), with an accumulation area of 337.3 km^2 and an Accumulation
348 Area Ratio (AAR) of 75.3%. The snowline reached its highest average elevation of $\sim 2550 \text{ m}$
349 a.s.l. in 2017, corresponding to an AAR of 68.4%. Even though some snowline measurements
350 were made early in the ablation season, we do not find our snowline measurements to be biased
351 by timing of the observation, as snowline elevations in the late melt season were not consistently
352 different from those early in the melt season (Figure 7a).



353
354 Figure 6. Donjek Glacier snowline. (a) Green box indicates extent of b, black outline shows
355 extent of Donjek Glacier on top of SPOT-5 DEM from 13 September, 2007. (b) Snowline from
356 1951 (blue) to 2017 (red). Satellite image from Landsat 8, 15 August, 2017.
357

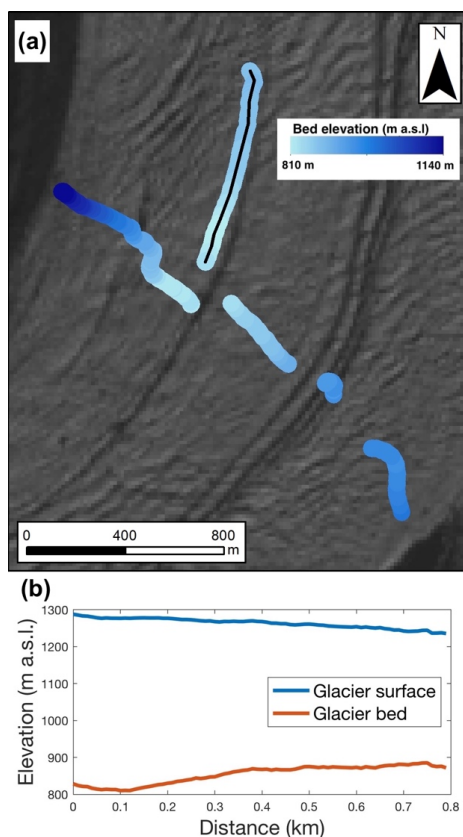


358
 359 Figure 7. Donjek Glacier climate. (a) Snowline measurements from the last available satellite
 360 image of each year in July (light blue), August (medium blue), and September (dark blue) with
 361 black error bars indicating one standard deviation. Red line shows linear trend for study period.
 362 (b) Burwash Landing annual average temperature record (red) with linear trend (thin red) and
 363 NARR temperatures from 1400-1600 m on Donjek Glacier from winter (light blue), summer
 364 (green), and annual mean (black) with linear trend (thin black). (c) Mean accumulation record
 365 from 1995, 2002, and 2016 ice cores from Eclipse Icefield (blue bars) with linear trend (red). (d)
 366 Rain from Burwash landing with annual (cyan) and monthly (black) totals from 1967 to 2012.
 367 Blue bars indicate a period when Donjek Glacier was known to surge, time periods found by
 368 Kochtitzky et al. (In Review).



369 4.4 Glacier geometry

370 Based on ground penetrating radar depth measurements downstream of the dynamic balance line
371 (8 km from glacier front; Fig. 1), we measured a bedrock rise towards the terminus (Figure 8).
372 Here, bedrock elevation rises from 810 to 890 m a.s.l. over a distance of 700 m in the
373 downstream direction, causing a 6.5° reverse bedrock slope (Figure 8), although the full spatial
374 extent of this reverse slope is unclear due to lack of measurements further down-glacier. The ice
375 thickness in this region ranges from 360 to 470 m, with deeper ice located closer to the dynamic
376 balance line.



377
378 Figure 8. (a) Donjek Glacier bed elevations in the reservoir zone, which indicate a reverse slope
379 towards the terminus. Base image: Landsat 8, 23 September, 2017. Extent of figure indicated by
380 green box in Figure 1a. (b) Profile for along-flow GPR transect of surface ice (blue) and bedrock
381 (red). Extent of profile indicated by black line in 7a.



382 4.5 Temperature and precipitation patterns

383 An increase in mean annual temperature of $\sim 0.05^{\circ}\text{C yr}^{-1}$ occurred at Burwash Landing between
384 1968 and 2017, equivalent to a total rise of $\sim 2.5^{\circ}\text{C}$ over the 50-year study period (Figure 7b),
385 which is consistent with the measured rise in snowline elevation. The mean annual temperature
386 at Burwash Landing reached a minimum of -6.9°C in 1973 and a maximum of 1.7°C in 2003. In
387 addition to mean annual temperature rise, the number of cumulative positive degree days at
388 Burwash Landing increased during each of the past four quiescent phases, from 15,095 PDD in
389 the 1967-1977 quiescent period to 18,899 PDD in the 2001-2012 period (Figure 4a).

390 Because Burwash Landing can frequently be impacted by winter time temperature
391 inversions and the temperature record has some missing data, we additionally examined the
392 temperature record from NARR for the 1400 to 1600 m elevation range of Donjek Glacier,
393 which corresponds to the area between $\sim 8 - 13$ km up glacier from the terminus. We find a
394 smaller rise in temperature of $\sim 0.02^{\circ}\text{C yr}^{-1}$ with an overall temperature rise of $\sim 0.65^{\circ}\text{C}$ over the
395 period 1979 - 2016. Given a rise in the snowline elevation of ~ 70 m, this suggests the NARR
396 temperature rise results are more accurate for Donjek Glacier compared to the temperature rise
397 observed at Burwash Landing.

398 Annual snow accumulation derived from the Eclipse Icefield ice cores shows no
399 significant trends over the study period, with values ranging from 0.62 to 1.91 m w.e. yr^{-1} (Fig.
400 7c). A linear fit to the annual average accumulation from 1948 to present has a non-significant
401 positive slope of 0.6 mm w.e. yr^{-1} (95% confidence). However, the accumulation variance has
402 increased from 0.039m^2 (1948 to 1982) to 0.068m^2 (1982 to 2016) in recent decades.

403 Precipitation records from Burwash Landing indicate that the initiation of the 1988, 2000,
404 and 2012 surges have coincided with several of the rainiest years on record, although not
405 necessarily high accumulation years (Figure 7d). The top five annual rainfall totals on record
406 from 1967 to 2012 for Burwash Landing were 2000 (293.5 mm), 2012 (284.0 mm), 1983 (274.9
407 mm), 1988 (273.9 mm), and 2005 (260.0 mm). However, the 1977 surge initiation coincided
408 with relatively dry conditions (27th highest annual total rainfall year in the study period) (Figure
409 7d). Days and/or months with higher total rainfall could have occurred while the station at
410 Burwash Landing was not operation.

411 Three of the top ten rainiest months appear to coincide with surge onsets (Figure 7d). The
412 rainiest month on record was July 1988 (131.8 mm) and Donjek started surging the following



413 month (Kochtitzky et al., In Review). The third rainiest month on record occurred in August
414 2000 (114.7 mm) and Donjek started to surge that month or the next (Kochtitzky et al., In
415 Review). Donjek surged at the end of the 1960s (Kochtitzky et al., In Review) and the tenth
416 rainiest month on record occurred in July 1967.

417 **5. Discussion**

418 **5.1 Snow and mass accumulation on surge-type glaciers**

419 The time it takes for a glacier to build up to its pre-surge geometry depends on the initial ice
420 volume displacement in the reservoir zone, the subsequent reservoir zone cumulative mass
421 balance, and the flux imbalance between actual and balance flux during quiescence (c.f. Clarke,
422 1987). Eisen et al. (2001) found that Variegated Glacier's cumulative mass balance consistently
423 reached a threshold of 43.5 m ice equivalent (39.9 m w.e.) before the glacier surged, while
424 Dyugеров et al. (1985) similarly found that a total of 360 ± 70 million tons of mass accumulated
425 between each of four surge events of Medvezhiy Glacier, Tajikistan. On Donjek Glacier, $15.5 \pm$
426 1.46 m w.e. or 16.6 ± 2.0 m w.e. accumulates at Eclipse Icefield between surge events,
427 dependent on whether we account for an offset in redistribution to the surge initiation region,
428 ~ 32 km downstream of the ice core site in Eclipse Icefield. For some glaciers, however, it is
429 known that during surges not all mass accumulated in the reservoir zone is emptied during a
430 subsequent surge: in Dyngjujökull, Iceland, for example, 13 km^3 of the 20 km^3 of ice
431 accumulated in the reservoir zone during its 20-year quiescence was transported to the receiving
432 zone in the 2 years of active surging (Björnsson et al., 2003). In addition, it is possible that the
433 consistent net accumulation observed at Eclipse Icefield between surge events simply reflects
434 consistent average accumulation (Wake et al., 2002; Kelsey et al., 2012) over each of the ~ 12 -
435 year surge intervals (Abe et al., 2015; Kochtitzky et al., In Review).

436 Surges of glacier systems with surge-type tributaries, or mass advection to or from
437 adjacent basins (e.g., outlets from ice caps), can be irregular, and it can be difficult to relate a
438 surge interval to climatic conditions and accumulation rates, even under quasi-stable climatic
439 conditions (Glazovskiy, 1996; Björnsson et al., 2003). One of Donjek Glacier's tributaries surged
440 in 2004 and 2010 (~ 23 km from its terminus on the east side of Donjek's main trunk, shown in
441 Fig. 1), adding mass to Donjek's main trunk ~ 2 km upstream of the top of the trunk's reservoir
442 zone (Kochtitzky et al., in review). However, even though both these tributary surges occurred in



443 the quiescent phase of the trunk glacier, the tributary surges do not seem to have shortened the
444 duration of the trunk's quiescent phases.

445

446 **5.2 Climate and surge behavior**

447 Surge-type glaciers occur preferentially, but not exclusively, in specific climate zones that are
448 bounded by temperature and precipitation thresholds (Sevestre and Benn, 2015). Temporal
449 changes in surge controls, and thus in surge propensity, can occur due to climate change or
450 climate-forced changes in glacier size, elevation, hypsometry, thermal regime and/or subglacial
451 drainage system. Glaciers have been observed to change their surge behavior to being less
452 vigorous or complete cessation in some regions (Hoinkes, 1969; Frappé and Clarke, 2007;
453 Hansen, 2003; Christoffersen et al., 2005; Clarke, 2014), while widespread renewed surge
454 activity has recently occurred in the high Karakoram (Hewitt, 2007; Copland et al., 2011;
455 Quincey et al., 2011; Bhambri et al., 2017). This suggests that mass balance, melt conditions,
456 thermal regime and related supra-, en- and subglacial hydrology may all influence surging (e.g.
457 Dowdeswell et al., 1995; Eisen et al., 2005; Sund et al., 2009).

458 Although temperature is increasing by 0.05°C per year at Burwash Landing, and Donjek
459 Glacier has a negative mass balance, we do not observe an altered surge recurrence interval. Ice
460 cores from Eclipse Icefield also show no significant change in precipitation since at least 1950
461 (Wake et al., 2002; Kelsey et al., 2012). However, Kochtitzky et al. (In Review) report that each
462 of the past 8 surges have been aerially less extensive than previous surge events, similar to other
463 glaciers in the St. Elias, such as Lowell Glacier (Bevington and Copland, 2014). Less extensive
464 surge events are likely caused by a rising snowline and increasing number of positive degree
465 days, leading to a persistently more negative mass balance (Berthier et al., 2010; Larsen et al.,
466 2015). Similar observations of less extensive surge events during a period of negative mass
467 balance have occurred in Iceland (Sigurdsson and Jónsson, 1995). These observations suggest
468 that glacier wide mass balance controls the intensity of each surge event, while other
469 mechanisms control the surge recurrence interval.

470 Rapid mass redistribution, related surface lowering, and frontal advance, during surges
471 are important for short- and long-term glacier surface mass balance. Post-surge accelerated
472 ablation, thinning and retreat rates have been measured and modeled for surge-type glaciers in
473 Iceland (Adalgeirsdottir et al., 2005), West Greenland (Yde and Knudsen, 2007), Alaska



474 (Muskett et al., 2008), and Svalbard (Nuttall et al., 1997; Moholdt et al., 2010). For Donjek
475 Glacier, surges lead to glacier-wide negative mass balance (Kochtitzky et al., In Review). While
476 many of these glaciers are already experiencing a negative mass balance (Larsen et al., 2015), the
477 enhanced negative mass balance associated with surging should be taken into account in
478 projections of glacier mass loss in a changing climate.

479

480 **5.3 Surge onset and weather**

481 Weather has been suggested to affect surge initiation and termination (Harrison and Post, 2003);
482 in particular, strong melt, heavy rainfall, and large annual accumulation rates. Here, we focus on
483 surge initiation, as our results show that three of the top ten rainiest months at Burwash Station
484 coincided with surge onsets of Donjek Glacier.

485 Lingle and Fatland (2003) postulated that a temperate glacier will not surge until it has
486 built-up critical thickness (basal shear stress), and surface meteorological conditions occur that
487 store a large volume of water englacially. For Alaskan-type surges this has been shown to result
488 in a late-winter to spring surge onset (Raymond, 1987; Harrison and Post, 2003). A suite of
489 anecdotal evidence supports this hypothesis (Kamb et al., 1985; Muskett et al., 2008; Pritchard et
490 al., 2005), but there are also examples of temperate glaciers with surge initiation in seasons other
491 than winter (Harrison et al., 1994; Björnsson et al., 2003), including Donjek Glacier. Because
492 Donjek Glacier surge initiation always initiates during summer months (Kochtitzky et al., 2019),
493 it appears that seasonality is important to initiate a Donjek surge event. Rainfall may play an
494 important role in this process.

495 Surge initiation in polythermal glaciers may not be as dependent on the influx of surface
496 meltwater, but rather on reaching a critical thickness combined with water trapped at the bed.
497 Although a spring start is also common for polythermal glaciers (Hodgkins, 1997; Jiskoot &
498 Juhlin, 2009), these surges can potentially start in any season and may therefore still involve
499 enhanced snow or rainfall (Quincey et al., 2011). Surge trigger zones in polythermal glaciers
500 have also been correlated with ponding of water and extensive slush flows associated with heavy
501 late-spring (wet) snowfalls alternated with short-term episodes of exceptionally high
502 temperatures (Hewitt, 2007). In summary, although some evidence and intuitive reasoning
503 suggest that the seasonality of surges could indeed be different for temperate glaciers than for



504 polythermal glaciers, no comprehensive analysis of seasonality of surge initiation and
505 termination in combination with thermal regime and surge development exists to date.
506

507 **5.4 Donjek surge mechanisms**

508 Abe et al. (2015) suggested that the constriction at 21 km from the terminus plays a
509 crucial role in causing Donjek Glacier to surge. However, Kochtitzky et al. (In Review) show
510 that the constriction was rather the upper extent of surge-type behavior, and in addition was
511 coincident with a change in bedrock lithology. We find no single conclusive factor that causes
512 Donjek Glacier to surge, although we can conclude that positive degree days are not a significant
513 control on surge recurrence interval. While Donjek Glacier reaches a consistent 13.1 to 17.1 m
514 w.e. accumulation before a surge event, this number cannot be confidently linked with the surge
515 recurrence interval given that it could also be an indicator of consistent decadal averaged
516 accumulation. Even though we show refilling of the reservoir zone on Donjek Glacier, limited
517 elevation measurements during recent surge events are inconclusive to use the reservoir zone as a
518 predictor for future surge events without more data. Assuming that past accumulation is an
519 indicator of future surge events, as displayed in Figure 4b, then the next surge is likely to occur
520 between 2022 and 2026.

521 More observations of Donjek Glacier surge kinematics, bedrock, and valley geometry are
522 needed to understand surging kinematics. While we show a bedrock rise beneath the dynamic
523 balance line, the relationship between the rise and surging is presently unclear. For a glacier in
524 the nearby Donjek Range, Flowers et al. (2011) suggest that its bedrock rise facilitates surging
525 because the reverse slope resists ice flow and promotes mass accumulation in the surge reservoir
526 zone during quiescence. Björnsson et al. (2003) conversely suggest from modeling results that
527 over-deepenings and reverse bed slopes enhance hydraulically inefficient subglacial drainage on
528 two surge-type glaciers in Iceland, diminishing mass accumulation. The role of the bedrock rise
529 in the surge behavior of Donjek Glacier is presently unknown, although it almost certainly plays
530 a role in controlling near-terminus ice dynamics, and thus is likely also involved in surge
531 dynamics.

532

533 **6. Summary and Conclusions**



534 We use three ice cores to reconstruct the accumulation record for Donjek Glacier leading up to
535 seven documented surge events since the 1930s. We find that Eclipse Icefield received between
536 13.1 and 17.7 m w.e. (mean of 15.5 ± 1.46 m w.e.) total accumulation between surge events.
537 While mean annual air temperatures increased by 2.5°C from 1968 to 2017 at Burwash Landing,
538 30 km from Donjek Glacier terminus, we observe no change in the surge recurrence interval over
539 this time period, although each recent surge advance has become less extensive than the
540 previous. Although we find that cumulative accumulation is the most consistent climate variable
541 between surge events of Donjek Glacier, our results remain inconclusive as to the role of
542 accumulation in driving surge behavior. We suggest that yet unknown subglacial processes,
543 possibly including changes in till deformation rates, are the primary driver of surging at Donjek
544 Glacier, but mass accumulation remains a necessary precondition for a surge to initiate.

545 Satellite glacier surface elevation measurements reveal rapid refilling of the surge
546 reservoir zone 8-21 km from the terminus of Donjek Glacier within the first 2 years following a
547 surge event. We find almost no reservoir zone refilling occurs in the 5 years leading up to a surge
548 event. The reservoir zone thickening is not the only cause of surge initiation, and therefore a
549 critical basal shear stress may need to be coincident with a hydrological switch. The highest
550 rainfall amounts typically occur during the summer month preceding a surge initiation. While not
551 every observed surge initiates with a high rainfall amount, the three most recent surges (1988-
552 1990, 2000-2002, 2012-2014) all coincide with one of the top five years on record for
553 precipitation.

554 Even though we observe a bedrock rise in the receiving zone of Donjek Glacier,
555 downstream of the dynamic balance line, the role that overdeepening and a reverse bedrock slope
556 play in surging of Donjek Glacier remains a crucial question. Further observations of bedrock
557 and bed elevation are necessary to understand surge mechanisms of Donjek Glacier. Monitoring
558 surface elevation changes on Donjek Glacier as it prepares for its next surge event by the mid-
559 2020s can yield valuable knowledge about how the subglacial hydrology beneath Donjek Glacier
560 changes as a surge initiates. This will ultimately lead to more knowledge of surge initiation
561 mechanisms, which can lead to better forecasting of surge events and magnitudes and therefore
562 mitigate glacier hazards.

563

564 **Author Contribution**



565 WK, KK, LC, and HJ designed the study. WK carried out data analysis for all remote sensing
566 and weather station data. DW, EM, KK, WK, and SC collected and analyzed the 2016 ice core.
567 DW, EM, KK, and WK reprocessed the 2002 ice core. LC, WK, BM, and CD collected glacier
568 thickness measurements. SW downscaled the NARR dataset and did all associated data analysis.
569 WK prepared the manuscript with contributions from all co-authors.

570

571 **Acknowledgements**

572

573 WK is supported by the National Science Foundation Graduate Research Fellowship under Grant
574 No. DGE-1144205. WK thanks Dan and Betty Churchill for funding the 2017 field season and
575 Geophysical Survey Systems, Inc. for funding the 2018 field season. LC thanks the Natural
576 Sciences and Engineering Research Council of Canada, University of Ottawa and Polar
577 Continental Shelf Program for funding and field logistics. KK thanks the NSF for funding St.
578 Elias research, NSF AGS-1502783. CD thanks the Canada Research Chairs Program, Natural
579 Sciences and Engineering Research Council of Canada, and Polar Continental Shelf Program for
580 funding and field logistics. WorldView DEMs provided by the Polar Geospatial Center under
581 NSF-OPP awards 1043681, 1559691, and 1542736. We thank Daniel Dixon, Steven Bernsen,
582 Justin Leavitt (UMaine), Dorota Medrzycka (uOttawa), and Patrick Saylor (Dartmouth College)
583 for their help collecting the 2016 ice core, Douglas Introne and Michael Handley for ice core
584 analysis, and Cameron Wake (University of New Hampshire) for help reprocessing the 2002
585 core isotope data. We thank Robert McNabb (uOslo) for the 2002 ASTER DEM and Icefield
586 Discovery, Trans North helicopters and the Kluane Lake Research Station for their logistical
587 support.

588

589 **References**

- 590 Abe T, Furuya M and Sakakibara D: Brief Communication: Twelve-year cyclic surging episodes
591 at Donjek Glacier in Yukon, Canada, *Cryosphere*10(4), 1427–1432, doi:10.5194/tc-10-
592 1427-2016, 2016.
- 593 Adalgeirsdóttir G, Björnsson H, Pálsson F and Magnússon E: Analyses of a surging outlet
594 glacier of Vatnajökull ice cap, Iceland. *Ann. Glaciol.* 42, 23–28,
595 doi:10.3189/172756405781812934, 2005.



- 596 Bhambri R, Hewitt K, Kawishwar P, Pratap B. Surge-type and surge-modified glaciers in the
597 Karakoram. *Scientific reports*, 7(1), p. 15391, 2017.
- 598 Berthier, E., Schiefer, E., Clarke, G. K. C., M'ennonos, B., and Remy, F.: Contribution of
599 Alaskan glaciers to sea-level rise derived from satellite imagery, *Nat. Geosci.*, 3, 92–95,
600 doi:10.1038/ngeo737, 2010.
- 601 Bevington A and Copland L: Characteristics of the last five surges of Lowell Glacier, Yukon,
602 Canada, since 1948, *J. Glaciol.* 60(219), 113–123, doi:10.3189/2014JoG13J134, 2014.
- 603 Björnsson, H., Pálsson, F., Sigurðsson, O.: Surges of glaciers in Iceland. *Annals of Glaciology*,
604 36: 82–90, 2003.
- 605 Bonifacio C, Barchyn TE, Hugenholtz CH, Kienzle SW.: CCDST: a free Canadian climate data
606 scraping tool, *Comput. Geosci.*, 75: 13–16. 10.1016/j.cageo.2014.10.010, 2015.
- 607 Budd, W.F.: A first model for periodically self-surging glaciers. *Journal of Glaciology*, 14 (70):
608 3-21, 1975.
- 609 Campbell, S., S. Roy, K. Kreutz, S. A. Arcone, E. C. Osterberg and P. Koons: Strain-rate
610 estimates for crevasse formation at an alpine ice divide: Mount Hunter, Alaska. *Annals of*
611 *Glaciology* 54(63): 200-208, doi:10.3189/2013AoG62A266, 2013.
- 612 Christoffersen, P., Piotrowski, J.A., Larsen, N.K.: Basal processes beneath an Arctic glacier and
613 their geomorphic imprint after a surge, Elisebreen, Svalbard. *Quaternary Research* 64,
614 125–137, 2005.
- 615 Clarke GKC and Mathews WH: Estimates of the Magnitude of Glacier Outburst Floods From
616 Lake Donjek, Yukon-Territory, Canada, *Can. J. Earth Sci.* 18(9), 1452–1463, 1981.
- 617 Clarke GKC, Schmok JP, Ommanney CSL and Collins SG: Characteristics of Surge-Type
618 Glaciers. *J. Geophys. Res. Solid Earth* 91(B7), 7165–7180, 1986.
- 619 Clarke, G.K.C.: Fast glacier flow: ice streams, surging, and tidewater glaciers. *Journal of*
620 *Geophysical Research*, 92 (B9): 8835-8841, 1987.
- 621 Clarke, GKC: A short and somewhat personal history of Yukon glacier studies in the Twentieth
622 Century. *Arctic* 67(1), 1-21, doi:10.14430/arctic4355, 2014.
- 623 Copland L and 7 others: Expanded and Recently Increased Glacier Surging in the Karakoram.
624 *Arct. Antarct. Alp. Res.* 43(4), 503–516, doi:10.1657/1938-4246-43.4.503, 2011.



- 625 Dansgaard W and Johnsen SJ: A Flow Model and a Time Scale for the Ice Core from Camp
626 Century, Greenland. *Journal of Glaciology* 8(53), 215–223,
627 doi:10.3189/S0022143000031208, 1969.
- 628 De Paoli, L., Flowers, G. E.: Dynamics of a small surge-type glacier investigated using 1-D
629 geophysical inversion. *Journal of Glaciology*, 55: 1101–1112, 2009.
- 630 Denton G. and Stuvier M.: Neoglacial Chronology, Northeastern St. Elias Mountains, Canada.
631 *Am. J. Sci.* 264, 577–599, 1966.
- 632 Dolgoushin LD and Osipova GB: Glacier surges and the problem of their forecasting. *IAHS-*
633 *AISH Publ.* 104, 292-304, 1975.
- 634 Dowdeswell JA, Hodgkins R, Nuttall A-M, Hagen JO and Hamilton GS: Mass balance change as
635 a control on the frequency and occurrence of glacier surges in Svalbard, Norwegian High
636 Arctic. *Geophys. Res. Lett.* 22(21), 2909–2912 doi:10.1029/95GL02821, 1995.
- 637 Dowdeswell, J.A., Hamilton, G.S., Hagen, J.O.: The duration of the active phase on surge-type
638 glaciers: contrasts between Svalbard and other regions. *Journal of Glaciology*, 37 (127):
639 338-400, 1991.
- 640 Dunse T and 5 others: Glacier-surge mechanisms promoted by hydro-thermodynamic feedback
641 to summer melt. *Cryosphere*, 9, 197–215 doi: 10.5194/tc-9-197-2015, 2015.
- 642 Dyurgerov, M. B., V. B. Aizin, and A. B. Buynitskiy: Nakopleniye massy v oblasti pitaniya
643 lednika Medvezh'yego za periody mezhdu yego podvizhkami [Mass accumulation in the
644 accumulation area of Medvezhiy Glacier during its quiescence periods]. *Mater. Glyatsiol.*
645 *Issled* 54, 131-135, 1985.
- 646 Eisen O., Harrison W.D. and Raymond C.F.: The surges of Variegated glacier, Alaska, U.S.A.,
647 and their connection to climate and mass balance. *J. Glaciol.* 47(158), 351–358
648 doi:10.3189/172756501781832179, 2001.
- 649 Eisen, O., Harrison, W.D., Raymond, C.F., Echelmeyer, K.A., Bender, G.A., Gordeev, V.V.:
650 Variegated Glacier, Alaska, USA: a century of surges. *Journal of Glaciology* 51 (174):
651 399-422, 2005.
- 652 Frappé, T., Clarke, G.K.C.: Slow surge of Trapridge Glacier, Yukon Territory, Canada. *Journal*
653 *of Geophysical Research*, 112, F03S32, doi:10.1029/2006JF000607, 2007.
- 654 Girod L, Nuth C, Kääb A, McNabb R and Galland O: MMASTER: Improved ASTER DEMs for
655 elevation change monitoring. *Remote Sens.* 9(7) doi:10.3390/rs9070704, 2017.



- 656 Glazovskiy, A.F.: The Problem of Surge-Type Glaciers. In: Kotlyakov (Ed). *Variations of Snow*
657 *and Ice in the past and at present on a Global and Regional Scale*. IHP-IV Project H-4.1,
658 UNESCO, 78pp, 1996.
- 659 Hansen, S.: From surge-type to non-surge-type glacier behaviour: midre Lóvenbreen, Svalbard,
660 *Annals of Glaciology*, 36: 97-102, 2003.
- 661 Harrison W.D. and Post A.: How much do we really know about glacier surging? *Ann.*
662 *Glaciol.*36(1), 1–6 doi:10.3189/172756403781816185, 2003.
- 663 Harrison, W.D., Echelmeyer, K.A., Chacho, E.F., Raymond, C.F., Benedict, R.J.: The 1987-88
664 surge of West Fork Glacier, Susitna, Alaska, U.S.A. *Journal of Glaciology*, 40 (135):
665 241-254, 1994.
- 666 Hewitt, K.: Tributary glacier surges: an exceptional concentration at Panmah Glacier, Karakoram
667 Himalaya. *Journal of Glaciology*, 53 (181): 181-188, 2007.
- 668 Hodgkins, R.: Glacier hydrology in Svalbard, Norwegian High Arctic. *Quat. Sci.*
669 *Rev.*, 16(9), 957–973, 1997.
- 670 Hoinkes, H.C.: Surges of the Vernagtferner in the Ötztal Alps since 1599. *Canadian Journal of*
671 *Earth Sciences*, 6: 853-860, 1969.
- 672 Jarosch, A.H., Anslow, F.S., Clarke, G.K.C.: High-resolution precipitation and temperature
673 downscaling for glacier models. *Clim. Dynam.*, 38, doi: 10.1007/s00382-010-0949-1, 2012.
- 674 Jiskoot, H., Juhlin, D.T.: Surge of a small East Greenland glacier, 2001-2007, suggests Svalbard-
675 type surge mechanism, *Journal of Glaciology*, 55(191): 567-570, 2009.
- 676 Jiskoot, H., Luckman, A., Murray, T.: Surge potential and drainage basin characteristics in East
677 Greenland. *Annals of Glaciology* 36, 142-148, 2003.
- 678 Johnson P.G.: The morphological effects of surges of the Donjek Glacier, St Elias Mountains,
679 Yukon Territory, Canada. *J. Glaciol.* 11(62), 227–234, 1972a.
- 680 Johnson P.G.: A possible advanced hypsithermal position of the Donjek Glacier, *Arctic* 25(4),
681 1972b.
- 682 Kamb, B., Raymond, C.F., Harrison, W.D., Engelhardt, H., Echelmeyer, K.A., Humphrey, N.,
683 Brugman, M.M., Pfeffer, T.: Glacier Surge Mechanism: 1982-1983 Surge of Variegated
684 Glacier, Alaska. *Science*, 227 (4686): 469-479, 1985.
- 685 Kaspari S, Hooke RLB, Mayewski PA, Kang S, Hou S and Qin D: Snow accumulation rate on
686 Qomolangma (Mount Everest), Himalaya: synchronicity with sites across the Tibetan



- 687 Plateau on 50–100 year timescales. *Journal of Glaciology* 54(185), 343–352,
688 doi:10.3189/002214308784886126, 2008
- 689 Kelsey, E.P., C.P. Wake, K. Yalcin, and K. Kreutz: Eclipse Ice Core Accumulation and Stable
690 Isotope Variability as an Indicator of North Pacific Climate. *J. Climate*, 25,6426–
691 6440, doi.org/10.1175/JCLI-D-11-00389.1, 2012.
- 692 Kochtitzky, W., Jiskoot, H., Copland, L., Enderlin, E., McNabb, R., Kreutz, K., and Main, B.:
693 Terminus advance, kinematics, and mass redistribution during eight surges of Donjek
694 Glacier, St. Elias Range, Canada, from 1935 to 2016. *Journal of Glaciology*, In Review.
- 695 Korona, J., E. Berthier, M. Bernard, F. Rémy, and E. Thouvenot: SPIRIT. SPOT 5 stereoscopic
696 survey of polar ice: Reference images and topographies during the fourth International
697 Polar Year (2007–2009), *ISPRS J. Photogramm. Remote Sens.*, 64, 204–212, 2009.
- 698 Larsen CF, Burgess E, Arendt AA, O’Neel S, Johnson AJ and Kienholz C.: Surface melt
699 dominates Alaska glacier mass balance. *Geophys. Res. Lett.*42(14), 5902–5908,
700 doi:10.1002/2015GL064349, 2015.
- 701 Lingle, C.S., Fatland, D.R.: Does englacial water storage drive temperate glacier surges? *Annals*
702 *of Glaciology*, 36: 14-20, 2003.
- 703 Meier M and Post A.: What are glacier surges? 6(4), 807–817 (doi:10.1139/e69-081)
- 704 Mesinger, F. et al. (2006). North American Regional Reanalysis. *Bull. Am. Meteorol. Soc.*, 87,
705 343-360, 1969.
- 706 Mingo, L., & Flowers, G.: An integrated lightweight ice-penetrating radar system. *Journal of*
707 *Glaciology*, 56(198), 709-714. doi:10.3189/002214310793146179, 2010.
- 708 Moholdt, G., Hagen, J. O., Eiken, T., and Schuler, T. V.: Geometric changes and mass balance of
709 the Austfonna ice cap, Svalbard, *The Cryosphere*, 4, 21-34, [https://doi.org/10.5194/tc-4-](https://doi.org/10.5194/tc-4-21-2010)
710 21-2010, 2010.
- 711 Murray, T., Strozzi, T., Luckman, A., Jiskoot, H., Christakos, P.: Is there a single surge
712 mechanism? Contrasts in dynamics between glacier surges in Svalbard and other regions,
713 *Journal of Geophysical Research*, 108(B5), 2237, doi: 10.1029/2002JB001906, 2003.
- 714 Muskett, R.R., C.S. Lingle, J.M. Sauber, A.S. Post, W.V. Tangborn, and Rabus B.T.: Surging,
715 accelerating surface lowering and volume reduction of the Malaspina Glacier system,
716 Alaska, USA, and Yukon, Canada, from 1972 to 2006. *Journal of Glaciology* 54(188),
717 788–800, 2008.



- 718 Nuth, C. and Kääb, A.: Co-registration and bias corrections of satellite elevation data sets for
719 quantifying glacier thickness change, *The Cryosphere*, 5, 271–290, doi:10.5194/tc-5-271-
720 2011, 2011.
- 721 Nuttall, A-M., Hagen, J.O., Dowdeswell, J.: Quiescent-phase changes in velocity and geometry
722 of Finsterwalderbreen, a surge-type glacier in Svalbard. *Annals of Glaciology*, 24: 249-
723 254, 1997.
- 724 Nye J.F.: Correction Factor for Accumulation Measured by the Thickness of the Annual Layers
725 in an Ice Sheet, *Journal of Glaciology* 4(36), 785–788 doi:10.3189/S0022143000028367,
726 1963.
- 727 Ohmura, A.: Physical basis for the temperature-based melt-index method. *Journal of applied*
728 *meteorology*, 40(4), 753-761, 2001.
- 729 Osipova, G.B., Tsvetkov, D.G.: Kinematics of the surface of a surging glacier (comparison of the
730 Medvezhiy and Variegated Glaciers). In: Kotlyakov, Ushakov, Glazovsky (Eds), *Glacier-*
731 *Ocean-Atmosphere Interactions*. IAHS Publications 208: 345-357, 1991.
- 732 Osterberg, E. C., P. A. Mayewski, D. A. Fisher, K. J. Kreutz, K. A. Maasch, S. B. Sneed, and E.
733 Kelsey: Mount Logan ice core record of tropical and solar influences on Aleutian Low
734 variability: 500–1998 A.D., *J. Geophys. Res. Atmos.*, 119, 11,189–11,204,
735 doi:10.1002/2014JD021847, 2014.
- 736 Pritchard, H., Murray, T., Luckman, A., Strozzi, T., Barr, S.: Glacier surge dynamics of
737 Sortebrae, east Greenland, from synthetic aperture radar feature tracking, *Journal of*
738 *Geophysical Research*, 110, F03005, doi:10.1029/2004JF000233, 2005.
- 739 Quincey, D.J., Braun, M., Bishop, M.P., Hewitt, K., Luckman, A.: Karakoram glacier surge
740 dynamics. *Geophysical Research Letters* 38, L18504, doi:10.1029/2011GL049004, 2011
- 741 Ragle, Richard H: "The Icefield Ranges Research Project, 1972." *Arctic* 26, no. 3: 258-63, 1973.
- 742 Raymond C.F.: How do glaciers surge? A review. *J. Geophys. Res.*92(1), 9121–9134, 1987.
- 743 RGI Consortium: Randolph Glacier Inventory – A Dataset of Global Glacier Outlines: Version
744 6.0: Technical Report, Global Land Ice Measurements from Space, Colorado, USA.
745 Digital Media. doi.org/10.7265/N5-RGI-60, 2017.
- 746 Robin, G. de Q. and Weertman, J.: Cyclic Surging of Glaciers. *Journal of Glaciology* 12(64), 3–
747 18, doi:10.3189/S002214300002267X, 1973.



- 748 Sevestre H and Benn DI (2015) Climatic and geometric controls on the global distribution of
749 surge-type glaciers: Implications for a unifying model of surging. *J. Glaciol.* 61(228),
750 646–662 (doi:10.3189/2015JoG14J136)
- 751 Shean DE and 6 others: An automated, open-source pipeline for mass production of digital
752 elevation models (DEMs) from very-high-resolution commercial stereo satellite imagery.
753 *ISPRS J. Photogramm. Remote Sens.* 116, 101–117, doi:10.1016/j.isprsjprs.2016.03.012,
754 2016.
- 755 Sigurdsson, O.: Variations of termini of glaciers in Iceland in recent centuries and their
756 connection with climate. In: Caseldine, C., Russell, A., Hardardóttir, J., Knudsen, Ó.
757 (Editors), *Iceland - Modern Processes and Past Environments. Developments in*
758 *Quaternary Science* 5, pp. 241-255, 2005.
- 759 Sigurdsson, O., Johnsson, T.: Relation of glacier variations to climate changes in Iceland. *Annals*
760 *of Glaciology* 21, 263-270, 1995.
- 761 Striberger, J., Björck, S., Benediktsson, I.O., Snowball, I., Uvo, C.B., Ingólfsson, O., Kjaer,
762 K.H.: Climatic control of the surge periodicity of an Icelandic outlet glacier. *Journal of*
763 *Quaternary Science* 26(6): 561–565, 2011.
- 764 Sund, M., Eiken, T., Hagen, J.O., Kääb, A.: Svalbard surge dynamics derived from geometric
765 changes. *Annals of Glaciology*, 50 (52): 50-60, 2009.
- 766 Tangborn, W.: Mass balance, runoff and surges of Bering Glacier, Alaska, *The Cryosphere*, 7,
767 867–875, doi:10.5194/tc-7-867- 2013, 2013.
- 768 Van Geffen, S. and Oerlemans, J.: The 1982/83 surge and antecedent quiescent phase of
769 Variegated Glacier: revising the original dataset for application in flow line
770 models, *Journal of Glaciology* 63(241), 772–782, doi:10.1017/jog.2017.43, 2017.
- 771 Van Wychen W and 5 others: Surface Velocities of Glaciers in Western Canada from Speckle-
772 Tracking of ALOS PALSAR and RADARSAT-2 data. *Can. J. Remote Sens.* 44(1), 57–
773 66, doi:10.1080/07038992.2018.1433529, 2018.
- 774 Wake CP, Yalcin K and Gundestrup NS: The climate signal recorded in the oxygen-isotope,
775 accumulation and major-ion time series from the Eclipse ice core, Yukon Territory,
776 Canada. *Annals of Glaciology* 35, 416–422, doi:10.3189/172756402781817266, 2002.
- 777 Williamson, S.N., Hik, D.S., Gamon, J.A., Jarosch, A.H., Anslow, F.S., Clarke, G., Rupp, S.:
778 Spring and summer monthly MODIS LST is inherently biased compared to air



- 779 temperature in snow covered sub-Arctic mountains, *Remote Sens. Environ.*, 189, 14-24,
780 2017.
- 781 Williamson, S.N., Anslow, F.S., Clarke, G.K.C., Gamon, J.A., Jarosch, A.H., Hik, D.S.: Spring
782 warming in Yukon mountains is not amplified by snow albedo feedback, *Nature*
783 *Scientific Reports*, 8, 9000, 2018.
- 784 Winski, D., Osterberg, E. F., Ferris, D., Kreutz, K., Wake, C., and Campbell, S.: Industrial-age
785 doubling of snow accumulation in the Alaska Range linked to tropical ocean warming.
786 *Nature Scientific Reports*, 7(1), 17869. <https://doi.org/10.1038/s41598-017-18022-5>,
787 2017.
- 788 Winstrup, M., Svensson, A. M., Rasmussen, S. O., Winther, O., Steig, E. J., and Axelrod, A. E.:
789 An automated approach for annual layer counting in ice cores, *Clim. Past*, 8, 1881–1895,
790 doi:10.5194/cp-8-1881-2012, 2012.
- 791 Yalcin K, Wake CP, Kang S, Kreutz KJ and Whitlow SI: Seasonal and spatial variability in
792 snow chemistry at Eclipse Icefield, Yukon, Canada, *Annals of Glaciology* 43, 230–238,
793 doi:10.3189/172756406781811998, 2006.
- 794 Yalcin, K., and Wake C.P.: Anthropogenic signals recorded in an ice core from Eclipse Icefield,
795 Yukon Territory, Canada, *Geophys. Res. Lett.*, 28, 4487–4490, 2001.
- 796 Yasunari, T. J., T. Shiraiwa, S. Kanamori, Y. Fujii, M. Igarashi, K. Yamazaki, C. S. Benson,
797 and T. Hondoh: Intra-annual variations in atmospheric dust and tritium in the North
798 Pacific region detected from an ice core from Mount Wrangell, Alaska, *J. Geophys.*
799 *Res.*, 112, D10208, doi:10.1029/2006JD008121, 2007.
- 800 Yde, J.C., Knudsen, N.T.: 20th-century glacier variations on Disko Island (Qeqertarsuaq),
801 Greenland. *Annals of Glaciology*, 46: 209–214, 2007.
- 802 Yde, J. C., Paasche, Ø.: Reconstructing climate change: Not all glaciers suitable, *Eos*
803 *Transactions AGU*, 91(21): 189–190, 2010.